Numerical Studies on Thin Wall Laminated Composite Hat-Stiffened Panels under Edge Compression Load

3.1 Introduction

Hat-stiffened panel can be applied extensively in defense, aircraft, automobiles area and structural applications. Hat-stiffened panel can be used as the load sharing walls of the compressive member in the structures and multi-storey buildings to reduce the dead load of the structure. FRP laminated panels have been currently used in bridge structure and heritage building for rehabilitation and retrofitting of structures due to its high strength and easy to place in the structures.

In this chapter, a parametric study has been carried out for optimizing smeared extensional stiffness ratio of stiffeners to that of skin of laminated composite hat-stiffened panel with the variation of pitch length stiffeners, depth of stiffeners and panel orthotropy ratio for three different plies configuration to maximize buckling capacity of the panel. Critical buckling load and global buckling mode shape of the laminated composite hat-stiffened panel are studied for the design of lightweight structures. Parametric studies of hat-stiffened panel under in-plane compressive load are presented with simply supported boundary conditions. Models are analyzed by applying Finite Element using ABAQUS. The design of laminated composite panel should be such that it can achieve better performance with specific strengths. Local buckling of the panel can be reduced by keeping depth of stiffener as small as possible and increasing number of the stiffeners.

Critical buckling load and global buckling mode shapes of the laminated composite hat-stiffened panel are studied here for the design of lightweight structures. Finite Element models of two different hat-stiffened (60^0-hat-stiffened and 75^0-hat-stiffened) panels have been analyzed by using ABAQUS and results have been critically compared. A database is provided by application of FE studies and on the basis of the study, few significant parameters of the buckling of laminated composite hat-stiffened panels under compressive loading are presented.

Many researchers have worked on parametrical studies of buckling of the laminated composite panel with blade type, I-shaped, J-shaped and T-shaped stiffeners in presence of in-plane shear, compression and combined loading, but the parametrical studies of buckling response of laminated composite panel with hat-stiffeners under compressive loading found less consideration. Ni et al. [2] presented a review of recent research based on two aspects application of finite element method (FEM) and experimental work with different loading conditions. For the design of the stiffened panel, computation of the stiffened panel is not efficient by using the numerical analysis due to the presence of a large number of variables in the panel.

The study of buckling of stiffened panels has limited available details under different loading conditions with blade-type, I-shaped, T-shaped and J-shaped stiffeners. Stroud and Anderson [4] studied the numerical formulation to find the buckling of blade type, hat-stiffeners, and corrugated stiffened panel. Smeared stiffeners technique is used to analyze the laminated composite panel subjected to various type of in plane loading with different of type stiffener [5]. Guo et al. [12] presented parametric studies of stiffened panels with variation of skin thickness to length ratios, ply configuration, stiffener depth to skin

thickness ratios and panel aspect ratios. Kalyanaraman and Upadhyay [40] discussed the behaviour of FRP box girders and proposed a computationally efficient method to study the single cell FRP box-girder bridges made with angle-shaped, T-shaped or blade-shaped stiffened panels using FEM based software ANSYS. Mallela and Upadhyay [41] presented parametrical study on the laminated composite stiffened panel under shear load with application of FEM. Rahimi et al. [43] analyzed the buckling response of shell structure due to stiffeners subjected to axial compressive load by ANSYS software. Huang et al. [45] computed the performance of stiffened panels using FE technique and arbitrated the accuracy of proposed model. Fathallah et al. [46] studied the optimization of ply orientation and number of layer of composite structure with T700/5505 Born and others laminated composite materials to find the minimum buoyancy factor for composite elliptical submersible pressure hull. Sudhirsastry et al. [47] performed the analysis of buckling of laminated stiffened panels with different shaped of stiffeners using ABAQUS based on FEM with carbon fiber and others composite materials. Square stiffened panel was fabricated with 8 layers of plate and 16 layers of different shaped of stiffeners. A parametric study is carried out to check the influence of geometrical parameters on the buckling load for different types of cylindrical stiffened composite panels under uniform in-plane periodic loads along the boundaries [71, 72]. Khedmati et al. [73] conducted a parametric study on stiffened panel to find the permissible spacing of intermittent fillet welds to prevent the local buckling of structural members and global buckling of the stiffened panel. Wodesenbet et al. [82] developed a smeared model to solve the buckling problem of a grid-stiffened composite cylinder by considering influence of moment and different types of geometric of the stiffeners.

3.2. Methodology for FE Modeling of Laminated Composite Hat-Stiffened Panels

3.2.1 Mathematical Formulation

The linear buckling analysis predicts the theoretical buckling capacity of an ideally linear elastic structure. On the other hand, the nonlinear buckling analysis develops a non-linear static analysis with gradually increasing loads to seek the load level at which the structure becomes unstable. Therefore, non-linear buckling analysis is efficient approach and it is recommended for the design of complex structural problems in civil engineering.
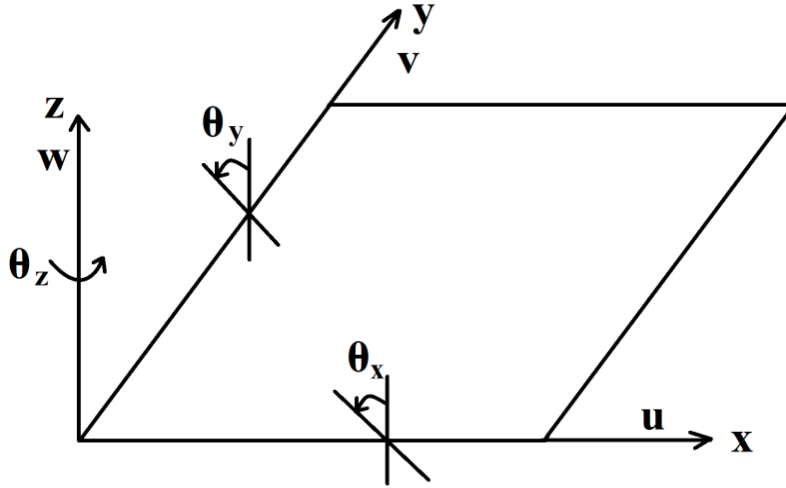
Figure 3.1 Displacement field and co-ordinate system

The reference system and the displacement field are shown in Figure 3.1, where the vectors u, v and w are the displacements along the x; y and z directions, and θ_x, θ_y and θ_z are the average rotations of a line initially perpendicular to the longitudinal plane. The displacements and the rotations within each element can be stated in terms of the nodal unknowns with the help of the shape functions (N_i), as given below

$$u = \sum_{i=1}^{n} N_i u_i \qquad v = \sum_{i=1}^{n} N_i v_i \qquad w = \sum_{i=1}^{n} N_i w_i \qquad (3.1)$$

$$\theta x = \sum_{i=1}^{n} N_i \theta x_i \qquad \theta y = \sum_{i=1}^{n} N_i \theta y_i \qquad \theta z = \sum_{i=1}^{n} N_i \theta z_i \qquad (3.2)$$

Where, n represents number of nodes of finite element.

In this work, four nodes S4R quadrilateral shell element has been considered for buckling analysis of stiffened panel. For each node, it is convenient to write the vector of unknowns as

$$\{q_i\} = \{ u_i, v_i, w_i, \theta x_i, \theta y_i, \theta z_i \}^T \tag{3.3}$$

The strain-displacement from the Mindlin-Reissner assumptions [9] as;

$$\{\epsilon\} = [B_0]\{q_i\} \tag{3.4}$$

Where, $[B_0]$ = strain-displacement matrix

The stress – strain relation can be determined from the constitutive law

$$\{\sigma\} = [C]\{\epsilon\} \tag{3.5}$$

Where, [C] matrix represents the material constant matrix.

The total potential energy V of the plate subjected to in-plane and transverse loading is the summation of the strain energy U and the work done by load W.

$$V = U-W = \int \{\sigma\}^T \varepsilon \, dv - \lambda \{q\}^T \{f\} \tag{3.6}$$

Where, λ is the single load factor to increment the load vector {f}.

As a first step, the linear buckling analysis is determined and needed for mathematical formulation of the stiffness matrix $[K_0]$ as given below

$$[K_0] = \int_V [B_0]^T [C][B_0]\,dv \tag{3.7}$$

Therefore, the pre-buckling solution can be found from

$$[K_0]\{q\} = \{f_0\} \tag{3.8}$$

In the second step, the critical stage along with fundamental path is determined. Therefore, it is needed to compute the geometric stiffness matrix $[K_\sigma]$ as given below [9]

$$[K_\sigma] = \int_V [G]^T [\sigma][G] dv \tag{3.9}$$

The linear eigenvalue problem is given by

$$([K_0] - \lambda[K_\sigma])\{x\} = \{0\} \tag{3.10}$$

The critical load λ^c can be determined from equation (3.10) and corresponding to Eigen vector $\{x\}$. The buckling analysis has been performed with various different parameters of two different types of hat-stiffener of the stiffened panel through FE models generated in ABAQUS.

3.2.2 FE Modeling in ABAQUS

The linear buckling analysis is performed for hat-stiffened panel under compressive loading by using a finite element software ABAQUS. Modeling of the laminated composite hat-stiffened panel is developed carefully to define the material properties of skin and stiffeners, number of layers, thickness and fiber orientation of the ply configuration. Shell element S4R is used for the analysis of panel, which possesses both bending and membrane capabilities. Uniformly distributed compressive loading of 1 kN/m is applied on the edge of the panel in stiffeners direction. The model has been submitted for the eigenvalue buckling analysis with application of simply supported boundary conditions on the panel. The buckling load has been obtained by multiplying the edge compressive load and the eigenvalue obtained from the FE analysis.

3.2.3 Validation Studies

The model of the hat-stiffened panel has been validated with results reported by Stroud et al. [5] which were obtained through the Engineering Analysis Language (EAL) on hat-stiffened panel of dimension 762 mm x 762 mm with six hat stiffeners. In the present study, 38.1 mm global size of the element has been taken for analysis of stiffened panel and the eigenvalue from the present study is in good agreement with EAL results of hat-stiffened panel as reported by Stroud et al. [5]. The hat-stiffened panel has been discretized with shell element (S4R) and 820 elements are generated of the panel as shown in Figure 3.2. The results from the present study has been found to be in good agreement with EAL results reported by Stroud et al. [5] for a panel under compression and combination of compression-shear and results are tabulated in Table 3.1. It has been found that the buckling mode shapes obtained are symmetrical for compression and combination of compression-shear, which is similar to the global buckling mode presented by Stroud et al. [5].
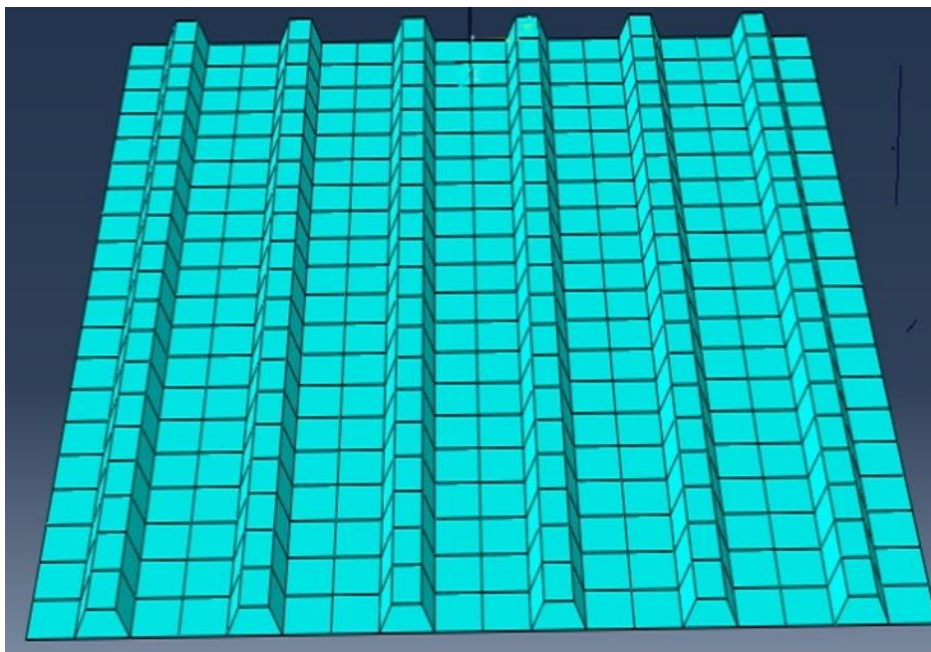
Figure 3.2 The hat-stiffened panel discretized with shell element (S4R)

Table 3.1 Validation of FE model

Applied load (kN/m)		FE analysis (eigen value)		% Difference $\left(\frac{b-a}{a}\right)*100$	FE analysis mode shape	
N_X	N_{XY}	Stroud et al. [5] (a)	Present study (b)		Stroud et al. [5]	Present study
175.1	0	3.0042	3.0158	0.38	Symmetric	Symmetric
175.1	175.1	2.3268	2.2386	-3.79	Symmetric	Symmetric

Table 3.2 Material properties of CFC used in the analysis (Sudhirsastry et al. [47])

Quantity	Symbol	Units	CFC materials
Young's modulus 0^0	E_{11}	GPa	164
Young's modulus 90^0	E_{22}	GPa	12.8
Shear modulus in plane 12 and 13	$G_{12=}G_{13}$	GPa	4.5
Shear modulus in plane 23	G_{23}	GPa	2.5
Poisson ratio in plane 12	υ_{12}	-	0.32
Ultimate tensile strength 0^0	X_{1t}	MPa	2724
Ultimate compressive strength 0^0	X_{1c}	MPa	111
Ultimate tensile strength 90^0	X_{2t}	MPa	50
Ultimate compressive strength 90^0	X_{2c}	MPa	1690
Ultimate shear strength in plane 12	S_{12}	MPa	120
Ultimate shear strength in plane 13	S_{13}	MPa	137
Ultimate shear strength in plane 23	S_{23}	MPa	60
Density	ρ	Kg/m^3	1800

3.3 Numerical Studies of the Panel

Numerical studies are carried out by analyzing the laminated composite hat-stiffened panel of dimension 762 mm x 762 mm under the edge compressive loading as shown in Figure 3 3. Pitch length of the stiffener is varied from 84.67 mm to 381 mm (number of the hat-stiffeners is varied 9 to 2 respectively) and depth (25 mm to 55 mm) of the stiffener with a fixed top width of 25 mm. Two different types of hat-stiffener (60^0-hat-stiffener and

75^0-hat-stiffener) are used for analysis of the panel. The carbon fiber composite (CFC) material property of each ply of thickness 0.125 mm is given in Table 3.2. Three types of ply configurations of skin are used for plate and stiffener component of the stiffened panel, which is given in Table 3.3.

Table 3.3 Ply configurations of elements of the panel

Skin of Panel component (Plate and stiffener)	Plies configuration	Each ply thickness (mm)	A_{11}/A_{22}	D_{11}/D_{22}
Skin – 1	$[[30^0/-30^0/90^0/0^0]_s]_s$	0.125	1.68	1.81
Skin – 2	$[[45^0/-45^0/90^0/0^0]_s]_s$	0.125	1.00	0.95
Skin – 3	$[[60^0/-60^0/90^0/0^0]_s]_s$	0.125	0.59	0.49
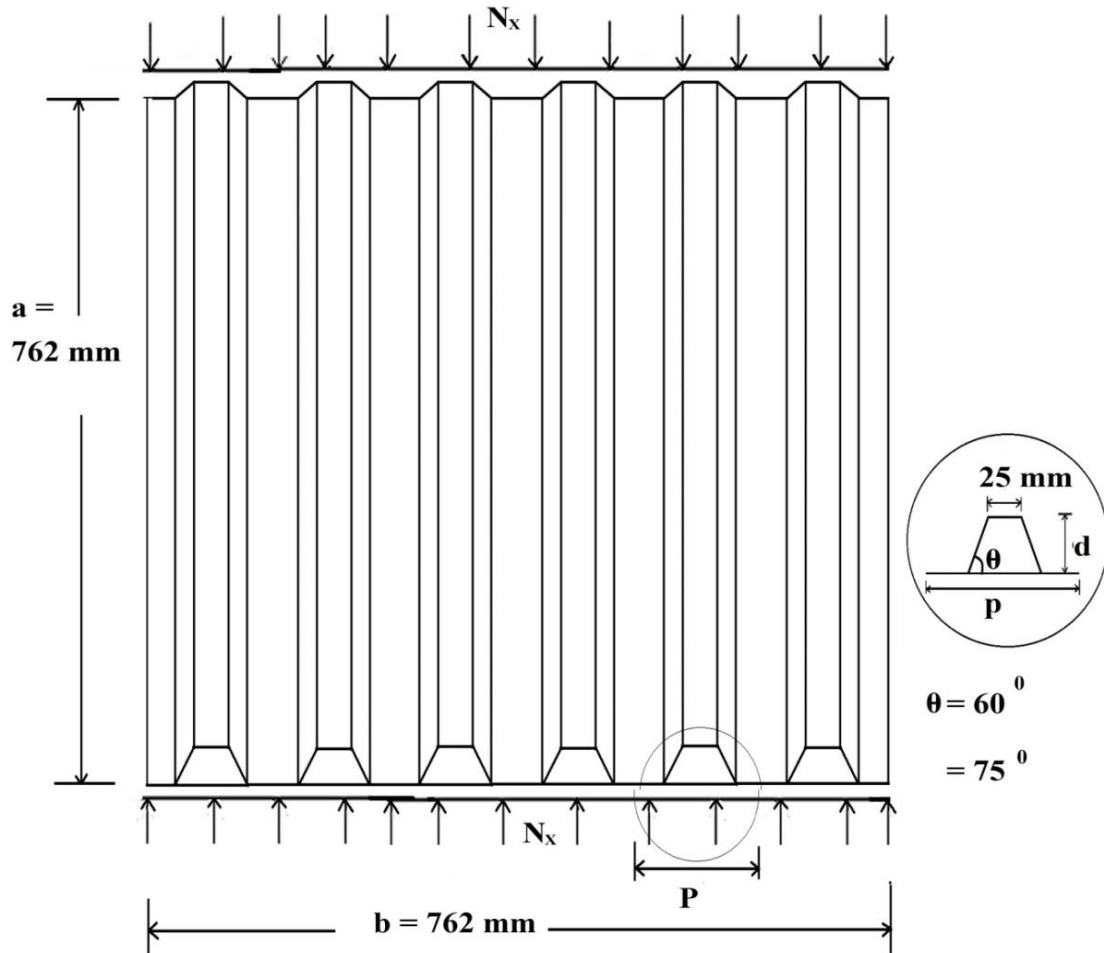
Figure 3.3 The structural geometry of hat-stiffened panel.

3.3.1 The Parameters

A program was developed in excel on the basis of smeared stiffness approach by using equations given below for different pre-decided orthotropy ratio with a variation of pitch length of stiffener for finding the corresponding hat-stiffener depth by trial and error for three different skins considered separately. The obtained depth of stiffener has been used for FE modeling of the stiffened panel. Table 3.4 and Table 3.6 show the cross-section in transverse direction of stiffener for 60^0-hat-stiffened and 75^0-hat-stiffened panel of different pitch length. Table 3.5 and Table 3.7 show the obtained depth by trial and error for three different skins considered separately for FE modeling of the 60^0-hat-stiffened and 75^0-hat-stiffened panel with fixed D_1/D_2.
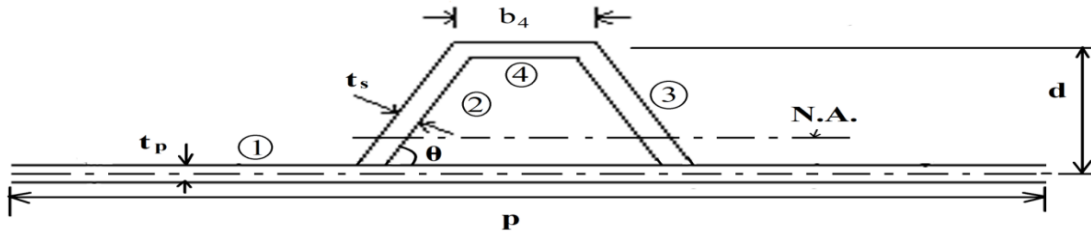
Figure 3.4 Cross-section of the hat-stiffener per pitch length with different elements.

D_1, D_2, and D_3 are the smeared orthotropic flexural stiffness in the longitudinal direction of stiffener, in transverse direction of stiffener and effective twisting stiffness of the panel respectively. The parameters of the stiffened panel have been identified from buckling differential equilibrium equation (3.11) based on classical laminated theory (Appendix-A) for symmetrical orthotropy material [4].

$$D_1 \frac{d^4 w}{dx^4} + 4D_3 \frac{d^4 w}{dx^2 dy^2} + D_2 \frac{d^4 w}{dy^4} + N_X \frac{d^2 w}{dx^2} = 0 \tag{3.11}$$

Where, N_X = buckling load of the panel, Stroud and Anderson [4] gave formulae for the smeared orthotropic flexural stiffness is given below.

Flexural stiffness of the panel (D_1) in the direction of stiffener is given as:

$$D_1 = \frac{1}{P} \sum_i \left(A_{11} - \frac{A_{12_i}^2}{A_{22_i}} \right) \left(b_i z_i^2 + \frac{b_i^3}{12} \sin^2\theta \right) + b_i D_{11_i} \cos^2\theta \tag{3.12}$$

Flexural stiffness of panel (D_2) in the direction transverse to stiffener is given as:

$$D_2 = (D_{22})_{\text{Plate}} \tag{3.13}$$

The smeared extensional stiffness of element per pitch is given as:

$$(EA)_i = \frac{1}{P} \sum_i \left(A_{11_i} - \frac{A_{12_i}^2}{A_{22_i}} \right) b_i \tag{3.14}$$

$\frac{(EA)_S}{(EA)_P}$ = smeared extensional stiffness ratio of stiffener to that of plate per pitch

Twisting stiffness of panel (D_3) per pitch is given as:

$$D_3 = D_3{}^\alpha + D_3{}^\beta \tag{3.15}$$

For open-section panels is given by

$$D_3{}^\alpha = \frac{1}{P} \sum_i b_i \left(\frac{1}{2} D_{12_i} + D_{66_i} \right) \tag{3.16}$$

For closed-section panels is given by

$$D_3{}^\beta = \frac{1}{P} \frac{\bar{A}^2}{\sum_i \frac{b_i}{A_{66_i}}} \tag{3.17}$$

Where,

    i = type of element of the panel [(Plate element is represented by '1') or different

        components of stiffener is represented by 2, 3, 4) as shown in Figure 3.4]

    b_i = width of the element, p = pitch length of the stiffener

    Z_i = distance from the neutral axis of the cross-section to the centroid of the element.

    Θ = inclination of the element with the horizontal direction.

    $\bar{A}$ = area enclosed by closed-section in one period.

    d = depth of the stiffener

Parameters and different components for hat-stiffened panel are calculated as follows:

(1) Orthotropy ratio of panel (D$_1$/D$_2$) for hat-stiffened panel:

Flexural stiffness of the panel (D$_1$) in the direction of stiffener is given as:

$$D_1 = \frac{1}{P} \Sigma_i \left(A_{11} - \frac{A_{12_i}^2}{A_{22_i}} \right) \left(b_i z_i^2 + \frac{b_i^3}{12} \sin^2\theta \right) + b_i D_{11_i} \cos^2\theta$$

$$= \frac{1}{P} \left[\begin{array}{c} \left[\left\{ \left(A_{11} - \frac{A_{12}^2}{A_{22}} \right)(b_1 z_1^2) + b_1 D_{11} \right\}_1 + \left\{ \left(A_{11} - \frac{A_{12}^2}{A_{22}} \right) \left(b_2 z_2^2 + \frac{b_2^3}{12}\sin^2\theta \right) + b_2 D_{11}\cos^2\theta \right\}_2 \right. \\ \left. + \left\{ \left(A_{11} - \frac{A_{12}^2}{A_{22}} \right) \left(b_3 z_3^2 + \frac{b_3^3}{12}\sin^2\theta \right) + b_3 D_{11}\cos^2\theta \right\}_3 + \left\{ \left(A_{11} - \frac{A_{12}^2}{A_{22}} \right)(p z_4^2) + p D_{11} \right\}_4 \right] \end{array} \right]$$

(3.18)

Flexural stiffness of panel (D$_2$) in the direction transverse to stiffener is obtain as:

D$_2$ = (D$_{22}$)$_{Plate}$

(2) $\dfrac{(EA)_S}{(EA)_P}$ = Smeared extensional stiffness ratio of stiffener to that plate per pitch:

(For given same skin of plate and stiffeners)

$$\frac{(EA)_S}{(EA)_P} = \frac{(b_2 + b_3 + b_4)}{P},$$

(3.19)

(3) (A$_{11}$ / A$_{22}$) = Ratio of extensional stiffness of skin

(4) D$_3$/D$_2$ of the panel:

Twisting stiffness of panel (D$_3$) per pitch, $D_3 = D_3^\alpha + D_3^\beta$

$$D_3 = \frac{1}{p} \left[2\{p - (b_4 + 2d\,Cot\theta)\}(0.5D_{12} + D_{66}) + \left\{ \frac{\overline{A}^2}{\dfrac{(b_2 + b_3 + b_4 + (b_4 + 2d\,Cot\theta))}{A_{66}}} \right\} \right]$$

(3.20)

b_i = width of the element:

$$b_1 = P$$

$$\left. \begin{array}{l} b_2 = b_3 = \dfrac{\left[d - \dfrac{(t_P + t_S)}{2} \right]}{Sin\theta} \\[2em] b_2 = \text{fixed width} = 25\,\text{mm} \end{array} \right\} \qquad (3.21)$$

Z_i = distance from the neutral axis of the cross-section to the centroid of the element:

$$\left. \begin{array}{l} Z_1 = \dfrac{\left(0 + 2t_S[d - \dfrac{(t_P + t_S)}{2}][(\dfrac{d}{2} - \dfrac{(t_S - t_P)}{4}] + b_4 t_S d \right)}{\left(pt_P + 2t_S[d - \dfrac{(t_P + t_S)}{2}] + b_4 t_S \right)} \\[3em] Z_2 = Z_3 = \left[\dfrac{d}{2} - \dfrac{(t_S - t_P)}{4} \right] - Z_1 \\[2em] Z_4 = d - Z_1 \end{array} \right\} \qquad (3.22)$$

The parameter is identified on the basis of generated data by trial and error which is influencing the buckling load of the panel. The parameter A_{11}/A_{22} is extensional stiffness in the longitudinal direction to the transverse direction of skin, D_1/D_2 gives the global flexural properties of panel, $(EA)_S/(EA)_P)$ gives the general concept about material strength of skin, and depth and pitch length of stiffener. The parameters D_1/D_2, and $(EA)_S/(EA)_P$ is increased upto a certain limit, which depends upon the skin of panel components (plate and stiffener), pitch length and depth of stiffener. For the given skin of panel, D_1/D_2 and $(EA)_S/(EA)_P$ of stiffened panel are increased only by increasing pitch length and depth of stiffener. Local buckling of the panel is increased with increasing the depth of stiffener. So that less depth of hat-stiffener is required to be used to reduce the local buckling of the stiffened panel.

Table 3.4 Cross-section of 60^0-hat-stiffened panel in transverse direction of stiffener for different pitch length

Pitch Length (P) (mm)	Cross-section of 60^0-hat-stiffened panel in transverse direction of stiffener
381	
254	
190.5	
127	
95.25	
84.67	
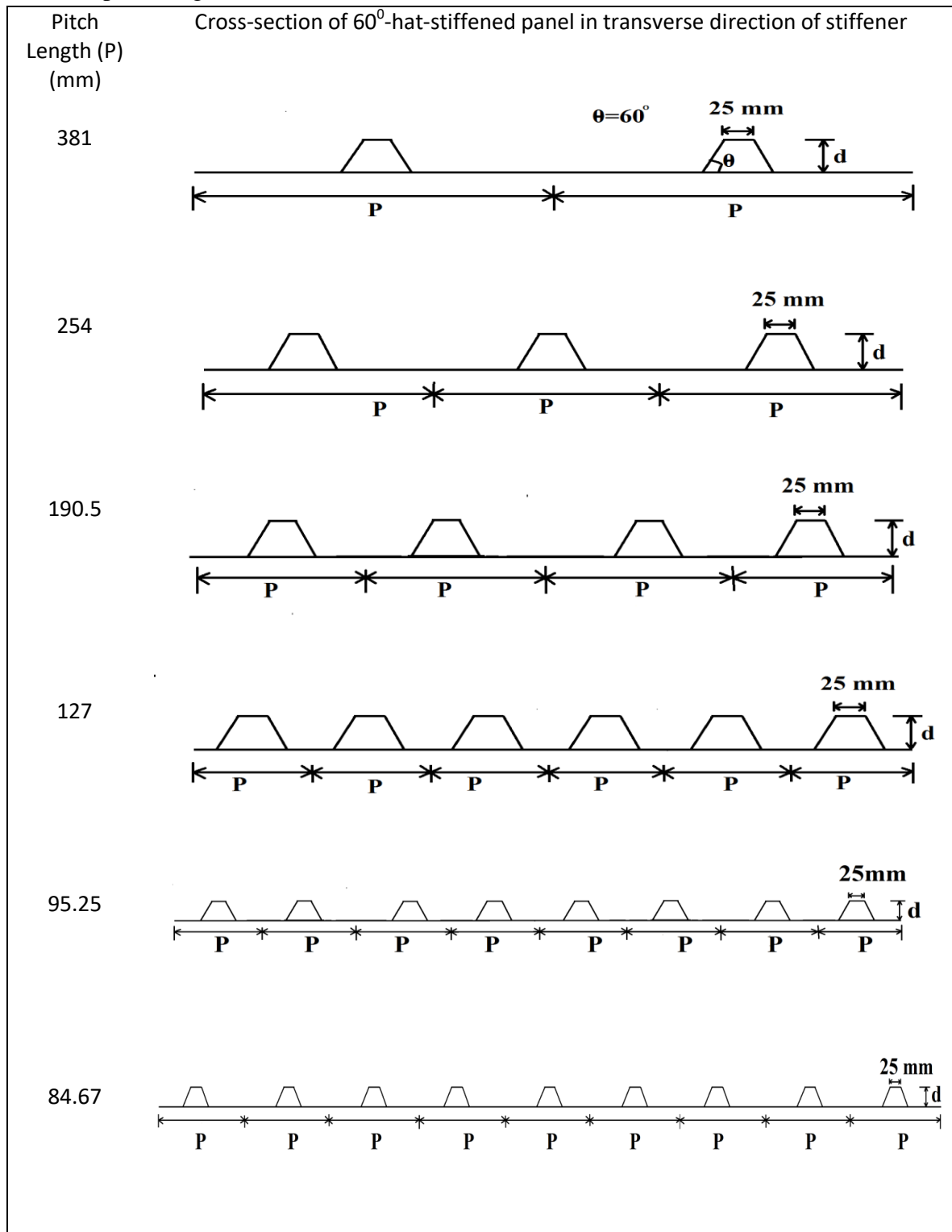
Table 3.5 Depth of stiffener based on smeared stiffness approach for FE modeling of the 60^0-hat-stiffened panel with fixed D_1/D_2.

D_1/D_2	Pitch Length (P) (mm)	Depth of stiffener (d) (mm)		
		Skin-1	Skin-2	Skin-3
100	381	15.340	20.210	25.330
	254	13.100	17.360	21.870
	190.5	11.733	15.620	19.750
	127	10.090	13.515	17.175
	95.25	9.100	12.245	15.615
	84.67	8.738	11.770	15.035
200	381	20.800	27.175	33.855
	254	17.880	23.505	29.430
	190.5	16.094	21.250	26.710
	127	13.933	18.510	23.387
	95.25	12.627	16.850	21.360
	84.67	12.144	16.230	20.605
300	381	24.746	32.200	40.000
	254	21.356	27.960	34.910
	190.5	19.277	25.350	31.770
	127	16.756	22.175	27.935
	95.25	15.230	20.236	25.580
	84.67	14.660	19.512	24.695
500	381	30.685	39.755	49.235
	254	26.614	34.690	43.180
	190.5	24.110	31.568	39.435
	127	21.064	27.750	34.836
	95.25	19.210	25.408	31.997
	84.67	18.516	24.528	30.925

Table 3.6 Cross-section of 75^0-hat-stiffened panel in transverse direction of stiffener for different pitch length

Pitch Length (P) (mm)	Cross-section of 75^0-hat-stiffened panel in transverse direction of stiffener
381	
254	
190.5	
127	
95.25	
84.67	
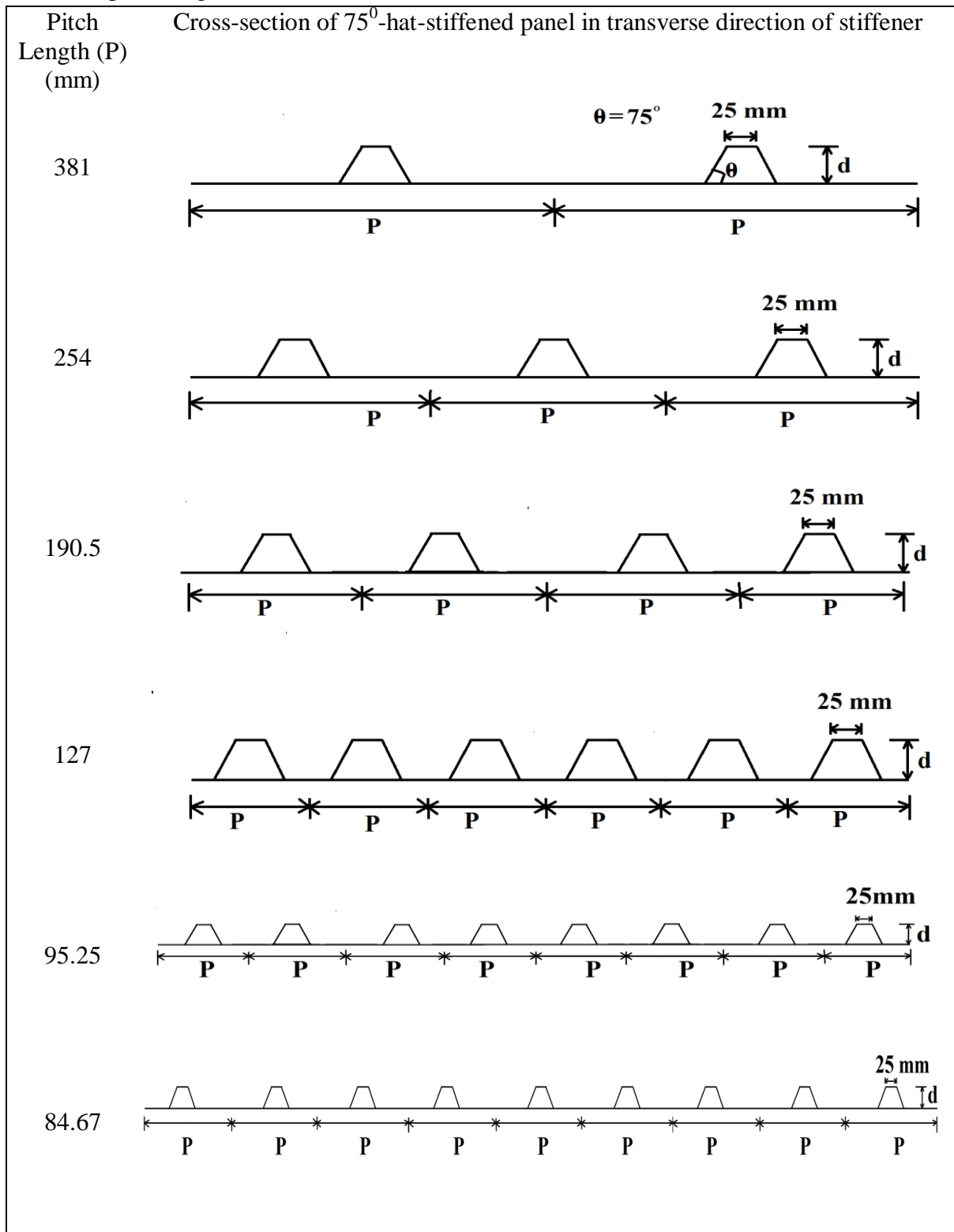
Table 3.7 Depth of stiffener based on smeared stiffness approach for FE modeling of the 75^0-hat-stiffened panel with fixed D_1/D_2.

D_1/D_2	Pitch Length (P) (mm)	Depth of stiffener (d) (mm)		
		Skin-1	Skin-2	Skin-3
100	381	15.510	20.480	25.710
	254	13.215	17.555	22.150
	190.5	11.820	15.770	19.970
	127	10.145	13.615	17.330
	95.25	9.146	12.320	15.735
	84.67	8.775	11.840	15.140
200	381	21.080	27.600	34.440
	254	18.080	23.820	29.875
	190.5	16.250	21.500	27.070
	127	14.040	18.690	23.650
	95.25	12.710	16.985	21.570
	84.67	12.215	16.354	20.792
300	381	25.115	32.750	40.745
	254	21.629	28.374	35.480
	190.5	19.492	25.685	32.240
	127	16.906	22.415	28.280
	95.25	15.345	20.426	25.860
	84.67	14.763	19.685	24.950
500	381	31.195	40.490	50.216
	254	26.996	35.255	43.945
	190.5	24.418	32.030	40.070
	127	21.286	28.095	35.323
	95.25	19.384	25.685	32.398
	84.67	18.674	24.782	31.295

The global buckling mode of 60^0-hat-stiffened panel under edge compression load is shown in Figure 3.5(a)-(b) for pitch length of 190.5 mm and 127 mm respectively. The global buckling mode of 75^0-hat-stiffened panel under edge compressive load is shown in Figure 3.6(a)-(b) for pitch length of 127 mm and 95.25 mm respectively.
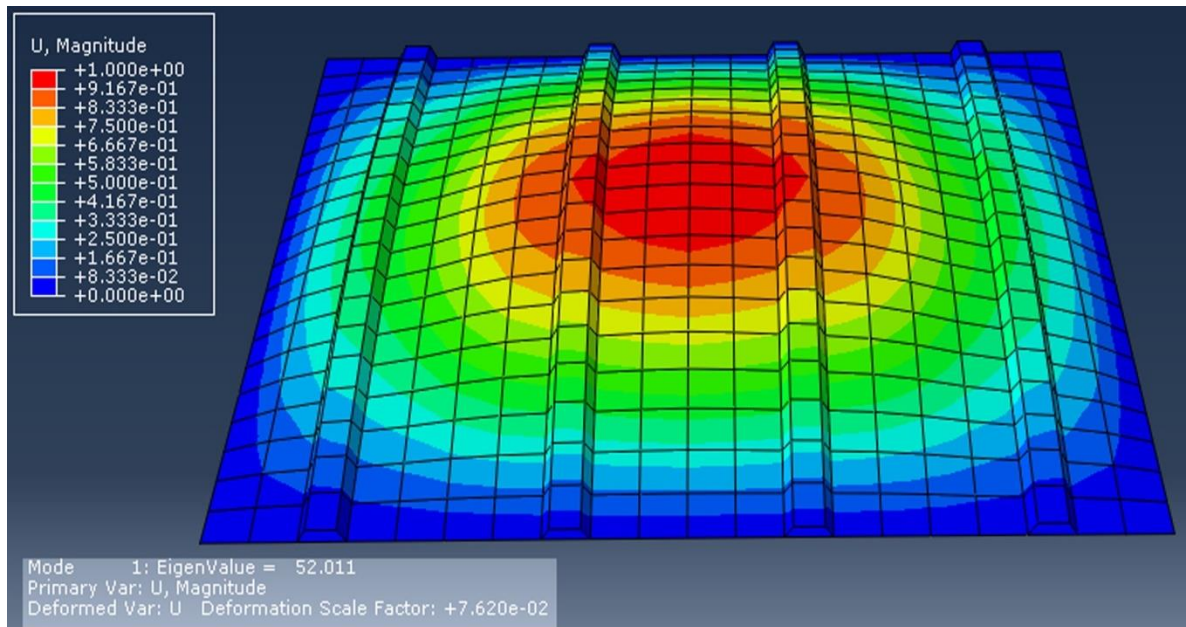
(a) pitch length = 190.5 mm with skin-1 for $D_1/D_2 = 100$
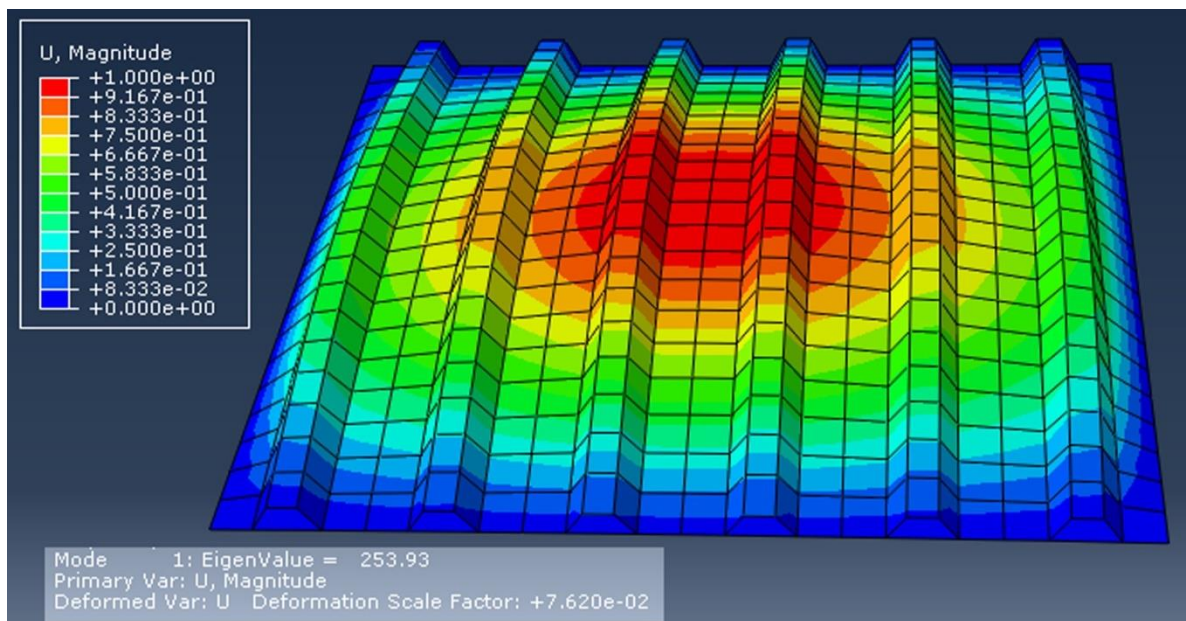
(b) pitch length = 127 mm with skin-2 for $D_1/D_2 = 500$

Figure 3.5 Global buckled mode shapes of 60^0-hat-stiffened panel
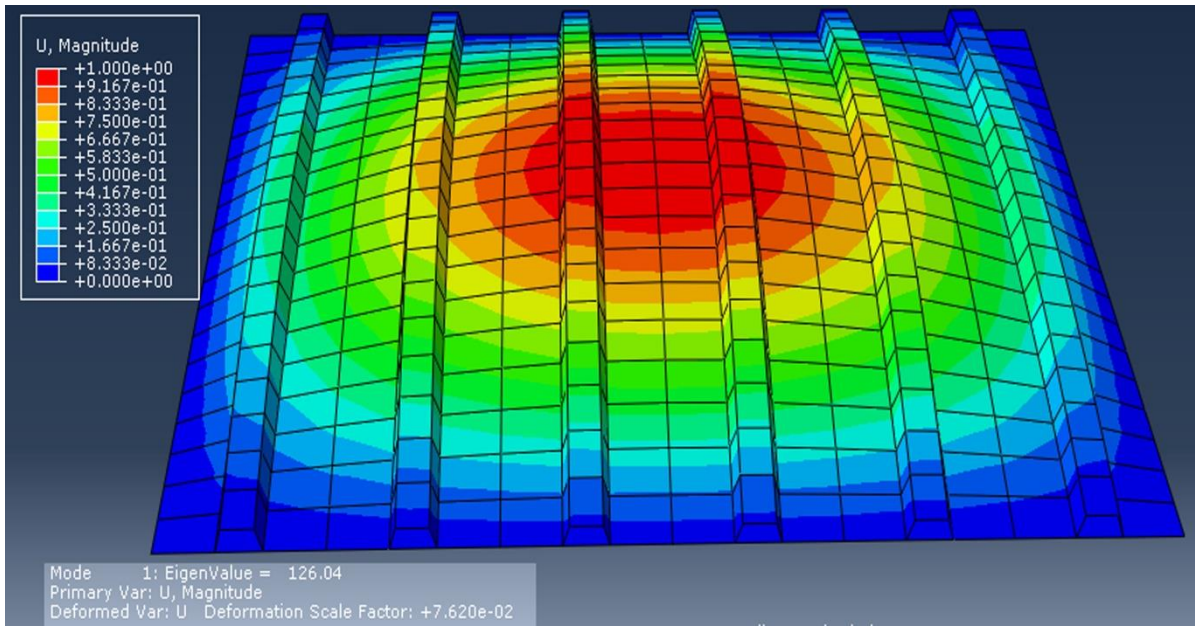
(a) pitch length = 127 mm with skin-2 for $D_1/D_2 = 200$
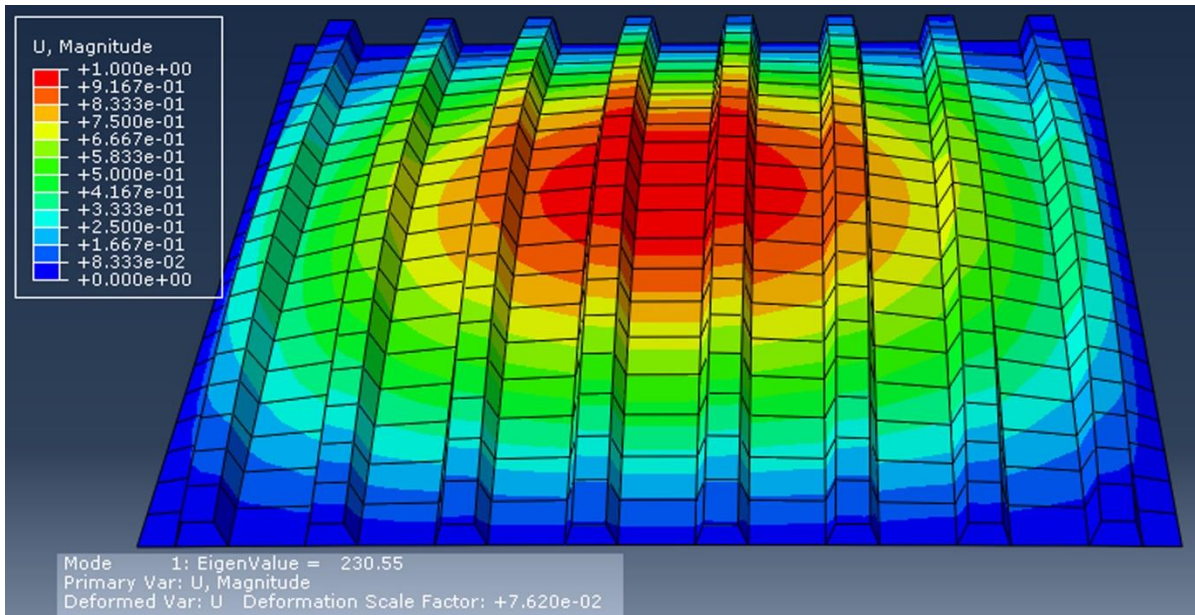
(b) pitch length = 95.25 mm with skin-3 for $D_1/D_2 = 300$

Figure 3.6 Global buckled mode shapes of 75^0-hat-stiffened panel.

3.4. Results and Discussion

Parameters affecting the buckling behaviour of hat-stiffened panel are identified on the basis of the generated database in the present study.

3.4.1 Influence of the Panel Orthotropy Ratio

For the different pitch lengths of the stiffener and the different skin, Figure 3.7(a)-(c) and Figure 3.8(a)-(c) show the variation of buckling load of hat-stiffened panels with D_1/D_2 of the 60^0-hat-stiffened and 75^0-hat-stiffened panel respectively. It is observed that the buckling load increases with the increasing D_1/D_2 in all cases of pitch lengths and all three types of skin for both 60^0-hat-stiffener and 75^0-hat-stiffener. Initially, buckling load increases with high rate but it is reduced further with increase of D_1/D_2. It is also observed that the buckling load of 60^0-hat-stiffener is greater than 75^0-hat-stiffener of the panel in all cases of given skins. For a given skin and D_1/D_2, the buckling load decreases with increasing pitch length of stiffeners. The 60^0-hat-stiffened panel with skin-3 has more buckling capacity in compression with all cases of skin and stiffener inclination. For the maximum buckling capacity hat-stiffened panel, 60^0-hat-stiffened panel is preferable with skin-3 and with lower pitch length of stiffener and greater D_1/D_2 as shown in Figure 3.7(c).

3.4.2 Influence of Smeared Extensional Stiffness Ratio of Stiffeners to that of Skin

For different D_1/D_2 and skin type, Figure 3.9(a)-(c) and Figure 3.10(a)-(c) show the variation of buckling load per unit area of the panels with $(EA)_S/(EA)_P$ of the 60^0-hat-stiffened and 75^0-hat-stiffened panel respectively. It is observed that with the increase in $(EA)_S/(EA)_P$, initially buckling load per unit area increases rapidly, after that it increases gradually and in the further it is approximately constant in all cases. This type of behaviour is more expressive in case of high D_1/D_2. The buckling load per unit area changes insignificantly with increase of $(EA)_S/(EA)_P$ in case of lower D_1/D_2. It is also observed that 60^0-hat-stiffener is more significant in comparison to 75^0-hat-stiffener in all cases of skin-type for the maximum buckling load per unit area.
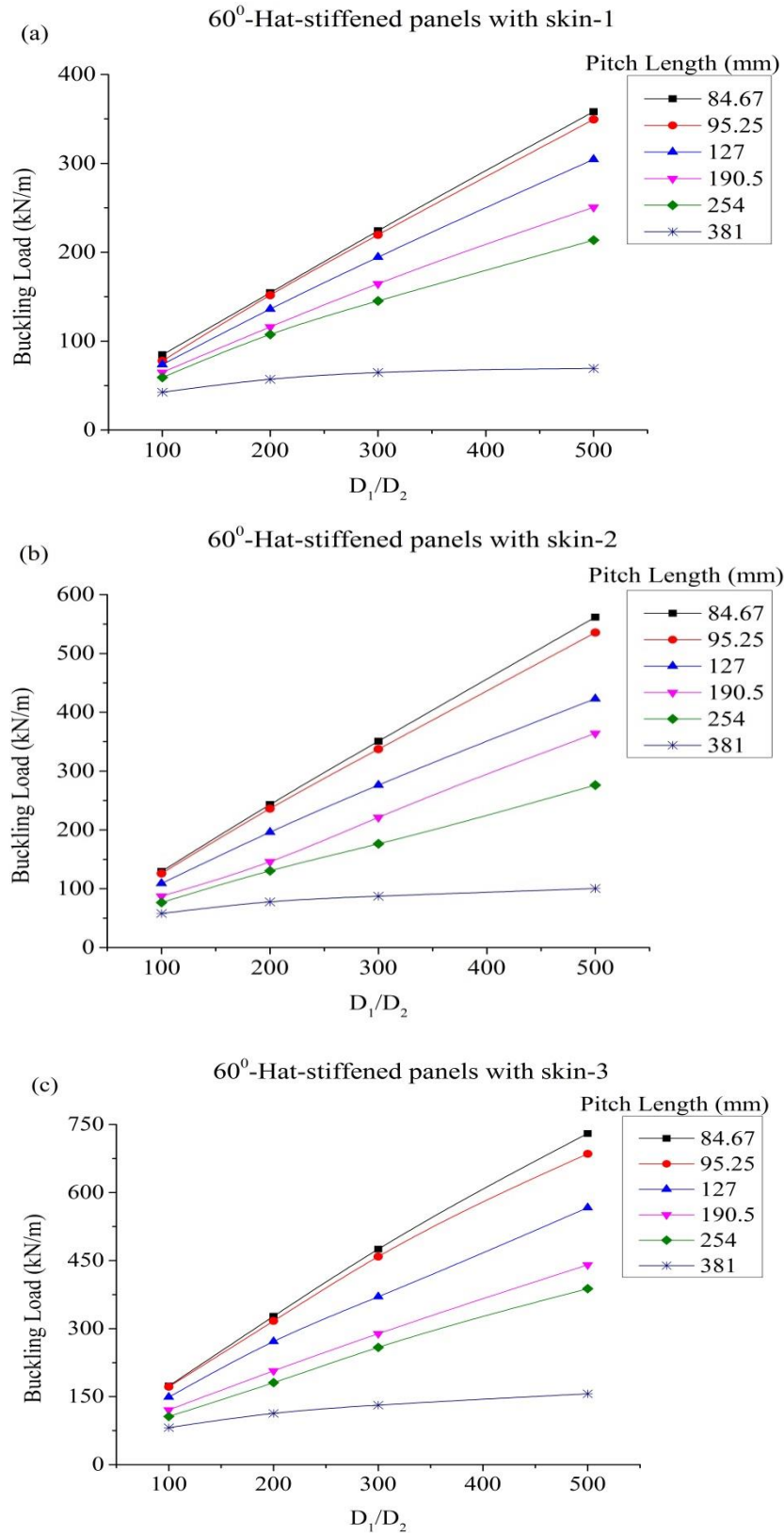
Figure 3.7 Buckling load of the 60^0-hat-stiffened panel with D_1/D_2 for different pitch length of stiffener and skin.
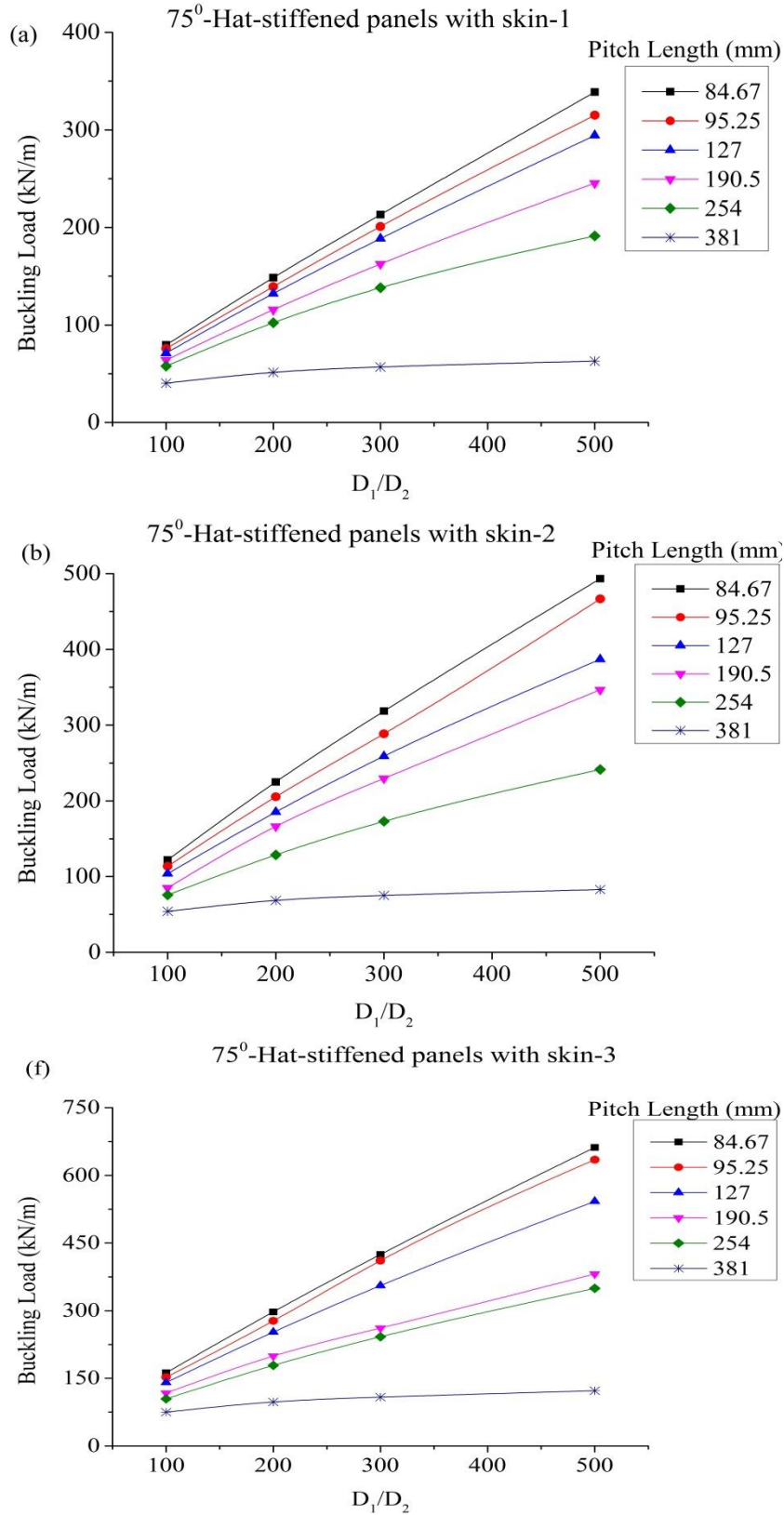
Figure 3.8 Buckling load of the 75^0-hat-stiffened panel with D_1/D_2 for different pitch length of stiffener and skin.

54
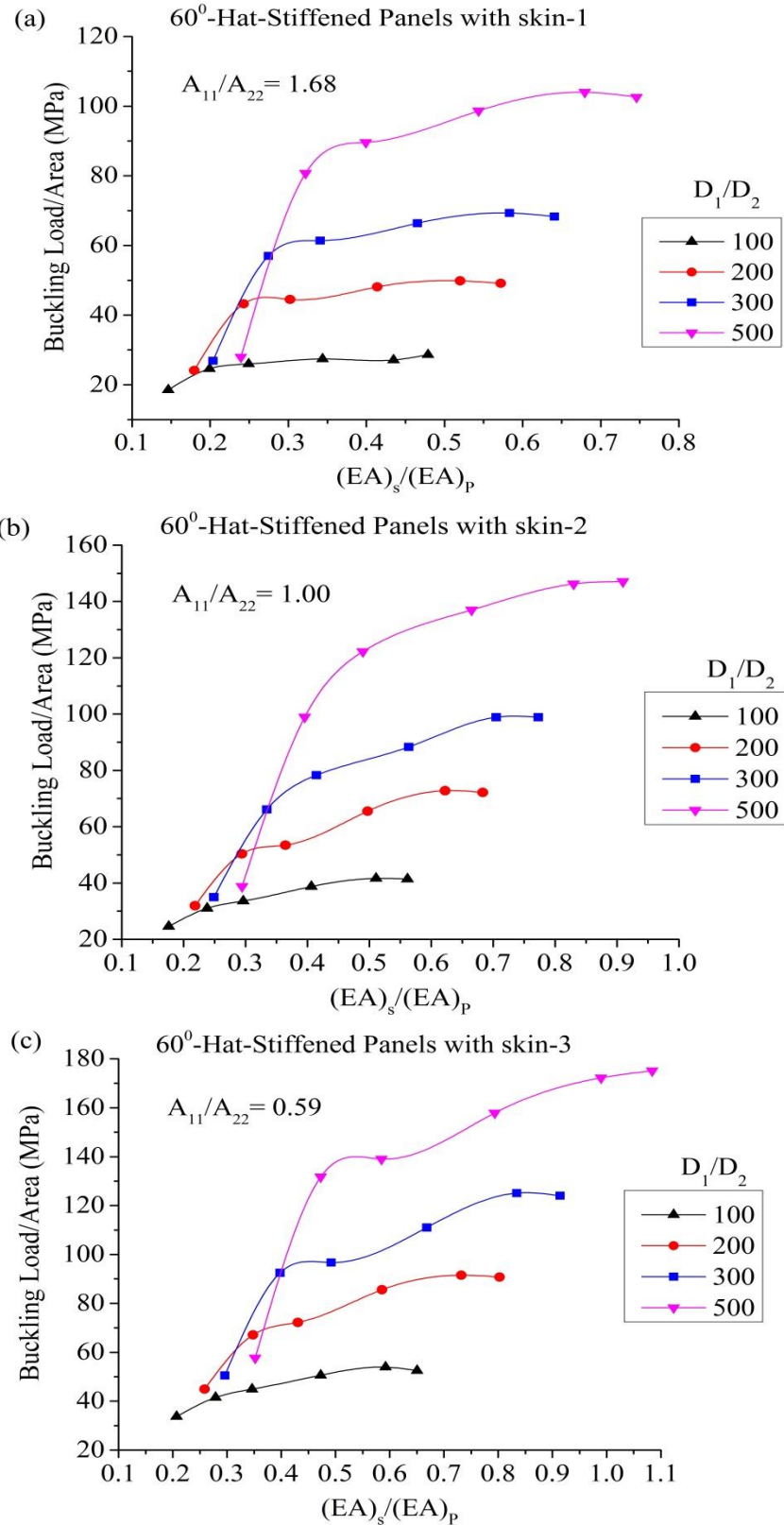
Figure 3.9 Buckling load/Area of the 60^0-hat-stiffened panel with $(EA)_S/(EA)_P$ for different D_1/D_2 and skin.

(a)

75⁰-Hat-Stiffened Panels with skin-1

$A_{11}/A_{22} = 1.68$

D_1/D_2
100
200
300
500

(b)

75⁰-Hat-Stiffened Panels with skin-2

$A_{11}/A_{22} = 1.00$

D_1/D_2
100
200
300
500

(c)

75⁰-Hat-Stiffened Panels with skin-3

$A_{11}/A_{22} = 0.59$
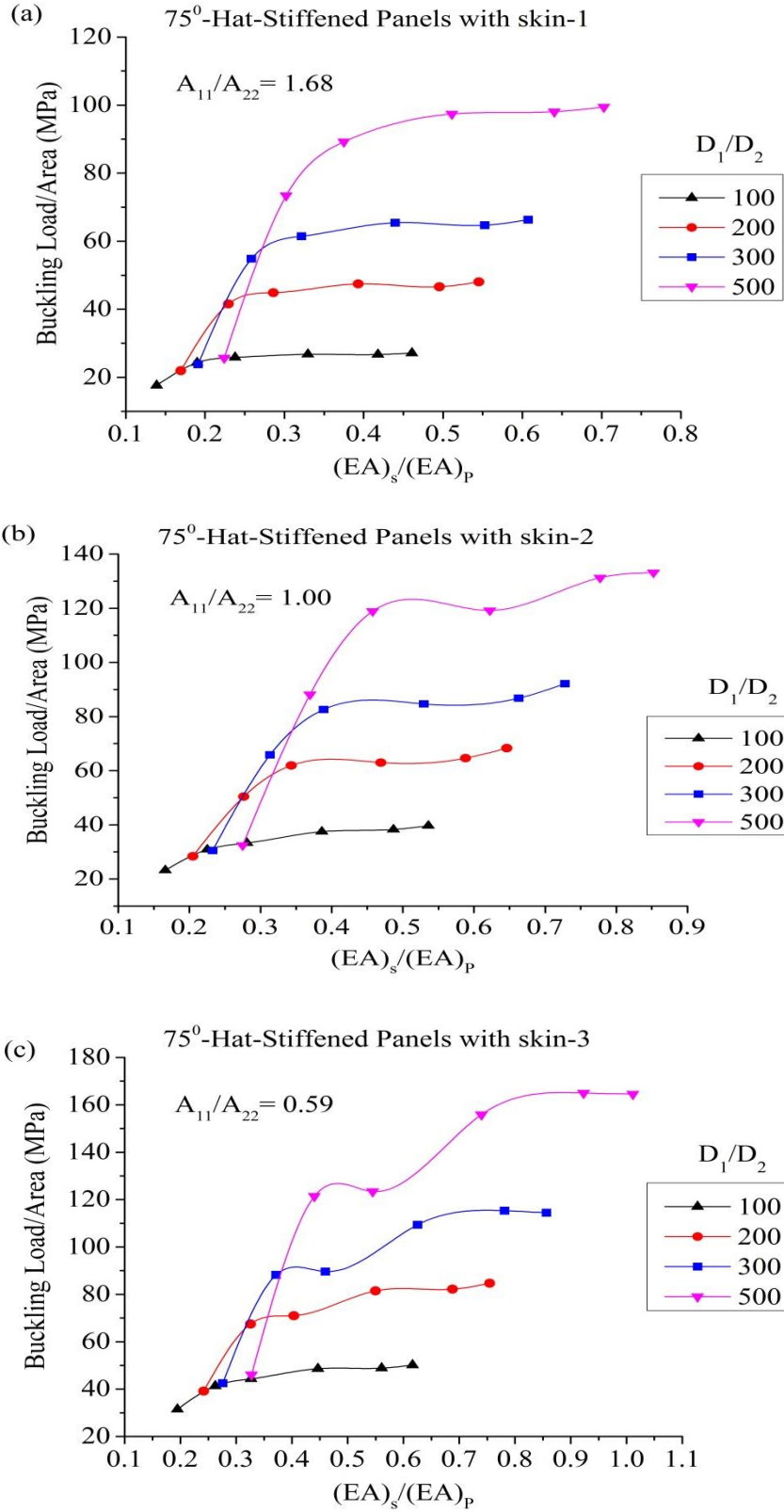
D_1/D_2
100
200
300
500

Figure 3.10 Buckling load/Area of the 75⁰-hat-stiffened panel with $(EA)_S/(EA)_P$ for different D_1/D_2 and skin.

In the above results, it has been found that the buckling load per unit area is increasing upto certain values of $(EA)_S/(EA)_P$ for all D_1/D_2 in different cases, after that buckling load per unit area is approximately constant. Further increasing the cross-section area of stiffener, buckling capacity per unit area of the hat-stiffened panel is not significantly improved with increasing $(EA)_S/(EA)_P$ and D_1/D_2. Therefore, $(EA)_S/(EA)_P$ and D_1/D_2 depend upon the depth and number of stiffeners for given skin. Hence, depth and number of stiffener of hat-stiffened panel is increased to certain limit for efficient buckling performance of panel without any increase in the weight of panel and the local buckling. In addition, local buckling of panel increases with increasing the depth of stiffener. Also it is to be noted that lesser depth of hat-stiffener of the panel is required to reduce the local buckling of the hat-stiffened panel.
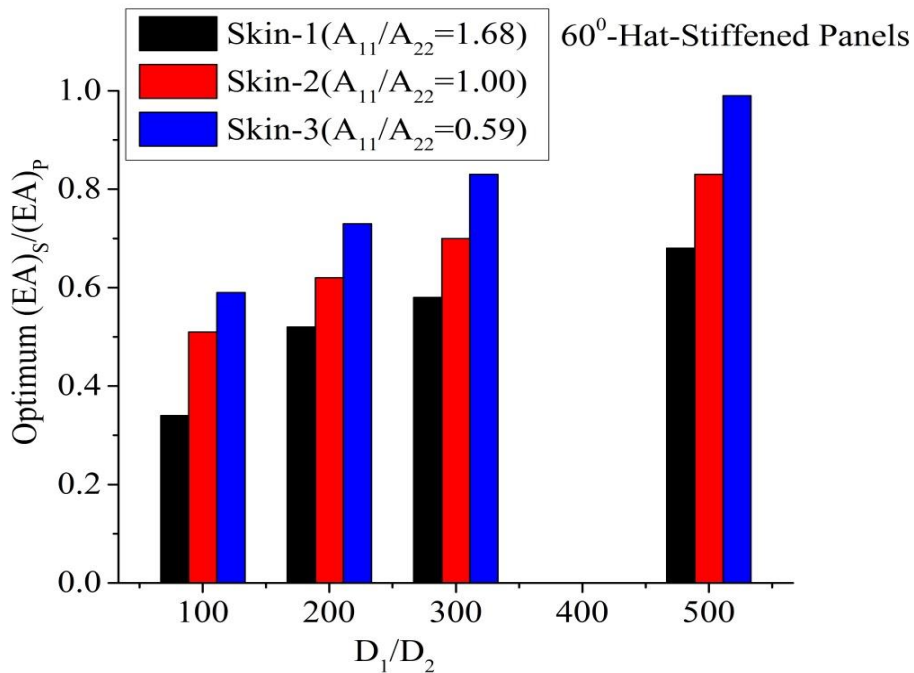
Figure 3.11 Optimum $(EA)_S/(EA)_P$ for different skin and D_1/D_2 for 60^0-hat-stiffened panel.
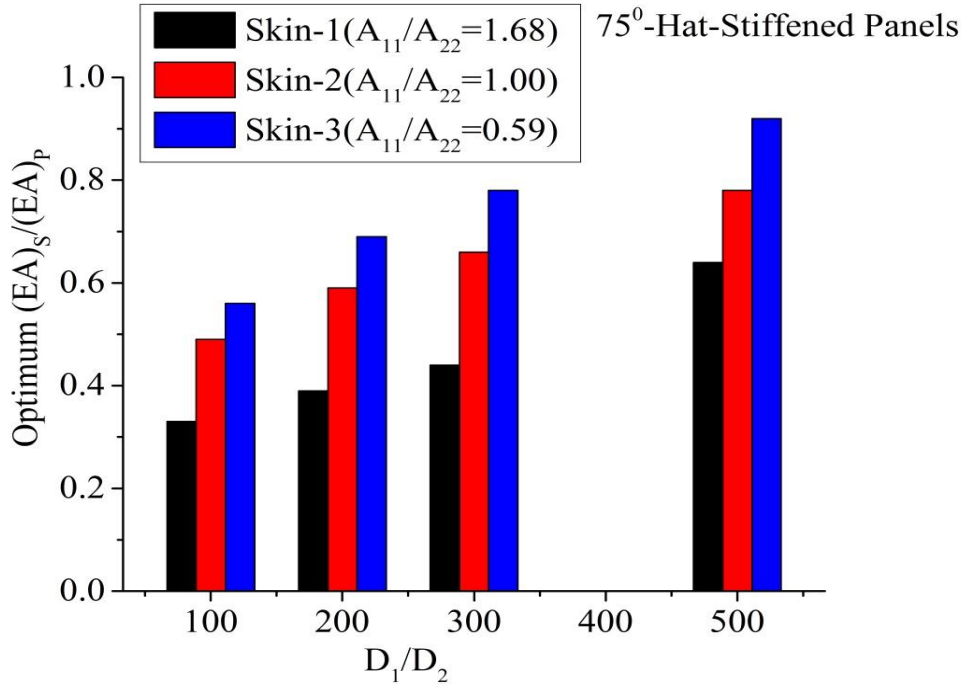
Figure 3.12 Optimum $(EA)_S/(EA)_P$ for different skin and D_1/D_2 for 75^0-hat-stiffened panel.

Ply configuration (skin-type) acts significantly in buckling performance of hat-stiffened panel. It affects the A_{11}/A_{22} ratio, which is significant for affecting the other parameters. In the present study, A_{11}/A_{22} for three different values 1.68 (skin-1), 1.00 (skin-2) and 0.59 (skin-3) is taken as shown in Table 3.3 for determination of buckling load of the panel. The minimum value of $(EA)_S/(EA)_P$ can be determined from Figure 3.9(a)-(c) and Figure 3.10(a)-(c) for all the different skins and D_1/D_2 at which the hat-stiffened panel has the maximum buckling load per unit area. This minimum value is defined as optimum $(EA)_S/(EA)_P$ of the hat-stiffened panel. Further, with increase of $(EA)_S/(EA)_P$, the buckling capacity per unit area curve becomes approximately constant.

The optimum $(EA)_S/(EA)_P$ is studied with variation of D_1/D_2 for different skin (A_{11}/A_{22}) of the panel as shown in Figure 3.11 and Figure 3.12 for 60^0-hat-stiffener and

75^0-hat-stiffener respectively. It is observed that the optimum $(EA)_S/(EA)_P$ increases with decreasing A_{11}/A_{22} for all different D_1/D_2. It is also observed that the optimum $(EA)_S/(EA)_P$ increases with D_1/D_2 for all the same skin. For skin-1 with increase of D_1/D_2 from 100 to 500, the optimum $(EA)_S/(EA)_P$ is varied from 0.34 to 0.68 with 60^0-hat-stiffened panel, and 0.33 to 0.64 with 75^0-hat-stiffened panel respectively. For skin-2 with increase of D_1/D_2 from 100 to 500, the optimum $(EA)_S/(EA)_P$ is varied from 0.51 to 0.83 with 60^0-hat-stiffened panel, and 0.49 to 0.78 with 75^0-hat-stiffened panel respectively. For skin-3 with increase of D_1/D_2 from 100 to 500, the optimum $(EA)_S/(EA)_P$ is varied 0.59 to 0.99 with 60^0-hat-stiffened panel, and 0.56 to 0.92 with 75^0-hat-stiffened panel respectively.

3.5 Summary

A novel numerical analysis of Linear buckling of the laminated composite hat-stiffened panel under edge compressive loading has been performed with different types of 60^0-hat-stiffeners and 75^0-hat-stiffeners. Parametric studies on buckling of the hat-stiffened panels have been conducted with variation of pitch length of stiffeners, number of stiffener, panel orthotropy ratio and smeared extensional stiffness ratio of stiffeners to that of skin with three different plies configuration. The 60^0-hat-stiffened panel is preferable for design of the maximum buckling capacity of the stiffened panel with less pitch length and greater D_1/D_2. The depth of hat-stiffener should be as small as possible to prevent the local buckling of the stiffened panel. The optimum $(EA)_S/(EA)_P$ increases with decreasing A_{11}/A_{22} for all different D_1/D_2 and it also increases with increasing D_1/D_2 for all similar skin for maximum buckling load per unit area of the panel. The 60^0-hat-stiffener shows significantly better performance in comparison to 75^0-hat-stiffener in all cases. For economical efficient design of the hat-stiffened panel, the pitch length and depth of the hat-

stiffener can be found with the help of optimum $(EA)_S/(EA)_P$ chart for different orthotropy

ratio D_1/D_2.